Catalysis Letters 54 (1998) 113–118

Methane coupling to acetylene over Pt-coated monoliths at millisecond contact times

K.L. Hohn, P.M. Witt, M.B. Davis and L.D. Schmidt

Department of Chemical Engineering, University of Minnesota, Minneapolis, MN 55414, USA

Received 5 February 1998; accepted 17 June 1998

We have studied the adiabatic and autothermal oxidative coupling of methane over Pt on α-Al_2O_3 monoliths at space velocities above 10^5 h^{-1}. The selectivity to C_2 hydrocarbons (primarily acetylene) reaches a maximum of around 20% at low fuel to oxygen ratios, low dilution, and high space velocities. These conditions promote a large temperature gradient in the monolith, with an exit temperature of nearly 1500 °C and an entrance temperature of less than 200 °C. This temperature gradient appears to be the driving force for C_2 hydrocarbon formation under these conditions. Both homogeneous and heterogeneous reactions may be involved in producing coupling products, and a combustion model predicts C_2 selectivities similar to those observed.

Keywords: methane coupling at low contact time, Pt monoliths

1. Introduction

The conversion of natural gas into value-added chemicals has received great attention in the last twenty years. Recent research has focused on converting CH_4, the major constituent of natural gas, into synthesis gas [1–3]. This is accomplished at long contact times by steam reforming,

$$CH_4 + H_2O \rightarrow CO + 3H_2 \qquad (1)$$

over Ni and at shorter contact times by partial oxidation,

$$CH_4 + (1/2)O_2 \rightarrow CO + 2H_2 \qquad (2)$$

over Rh [2,4–8]. Synthesis gas can then be converted to higher hydrocarbons through Fischer-Tropsch chemistry [9] or to methanol.

It has also been shown that CH_4 can be converted to C_2's directly by oxidative coupling [10,11] or homologation [12,13]. In oxidative coupling, CH_4 and O_2 are fed over a metal or metal oxide catalyst at moderate temperatures (500–800 °C) to produce mainly ethylene. Selectivities in excess of 80% have been reported with CH_4 conversions around 20%. The first major study of oxidative coupling was done by Keller and Bhasin in 1982 [14]. They investigated numerous metals and found that Pt was not active for coupling. Since then, considerable work has focused on oxidative coupling, particularly on metal oxides, and several review articles have been published on this subject [10,11,15–17]. In homologation, pure CH_4 is passed over a noble metal catalyst to produce a carbon layer. Then H_2 is substituted for CH_4 to remove the carbon as higher hydrocarbons.

Recently we reported that significant methane oxidative coupling could be achieved over Rh-coated α-Al_2O_3 ceramic monoliths [8]. As the gas hourly space velocity (GHSV) increased, the selectivity to C_2's increased until O_2 breakthrough occurred. Above a GHSV of 5×10^5 h^{-1} all C_2 products disappeared. By preheating the feed gas and decreasing the CH_4/O_2 ratio C_2 selectivities as high as 10% were achieved on Rh. An important feature of this work is the temperature profile across the monolith catalyst. At high GHSV the entrance of the catalyst is cold, approximately 200 °C, while the exit temperature is almost 1500 °C. It was suggested that this temperature profile allows for the production of coupling products which were not seen ($<$0.5%) in previous research carried out at lower space velocities [14].

We previously reported that Pt, while not a highly selective catalyst for syngas, is more selective than Rh for the production of olefins from light alkanes [18–20]. By replacing Rh with Pt, we find that the coupling selectivity can be improved to at least 20%.

2. Experimental

Catalysts were prepared as detailed previously [18]. Ceramic foam α-Al_2O_3 monoliths (18 mm diameter, 10 mm long, 45 pores per linear inch) were saturated with an aqueous solution of H_2PtCl_6 and dried overnight. The catalysts were then calcined in air at 600 °C and reduced at the same temperature in H_2. Metal loadings were 2–3% Pt by weight.

Experiments were carried out in a quartz tube reactor 18 mm diameter and 40 cm long. Uncoated ceramic monoliths were positioned before and after the catalyst to reduce axial radiation losses. The monoliths were sealed in the reactor with high-temperature cloth to prevent gas bypass. The outside of the reactor was wrapped with insulation to closely approximate adiabatic operation. The temperature of the catalyst was measured with a Pt/13% Rh thermocouple placed at the exit and a chromel/alumel thermocouple located at the entrance of the catalyst. The catalysts were ignited with a Bunsen burner at a CH_4/O_2 ratio of 1.7 and a flow rate of 3 standard liters per minute (slpm).

Reactant gases were controlled by mass flow controllers with an accuracy of ±0.01 slpm. The CH_4/O_2 ratio was held constant at 1.7, and N_2 dilution remained constant at 20% for all experiments unless otherwise stated.

Product gas compositions were measured with an HP 5890 gas chromatograph equipped with thermal conductivity and flame ionization detectors and integrated by an online computer. Products detected include H_2, CO, CO_2, H_2O, C_2H_6, C_2H_4, C_2H_2 and C_3 and C_4 hydrocarbons. Methane conversion and product selectivities are determined from molar flow rates as described previously [2] and all mass balances closed within ±5%.

3. Results

3.1. Flow rate

The conversion of O_2 and CH_4 along with the entrance and exit temperature of the catalyst are shown in figure 1 as a function of gas hourly space velocity (h^{-1}) for Rh (upper panel) and Pt (lower panel) at $CH_4/O_2 = 1.7$. On rhodium, CH_4 conversion falls from over 80% at GHSV of 2×10^5 h^{-1} to around 30% at GHSV of 9×10^5 h^{-1}. The oxygen conversion also falls with increasing GHSV, falling from almost 100% to only 60% at GHSV of 9×10^5 h^{-1}. Coupling selectivity increases from less than 0.1% to almost 5% at GHSV of 4×10^5 h^{-1} before falling to less than 0.1% at the highest space velocities. On Pt, the O_2 and CH_4 conversions remain constant at 100 and 62%, respectively. As the GHSV increases to 3.5×10^5 h^{-1}, the exit temperature increases from 1100 to 1500 °C and the entrance temperature decreases from 800 to 200 °C. The total selectivity to coupling products is also shown in figure 1. The coupling selectivity increases from 10% at 10^5 h^{-1} to approximately 20% at a GHSV of 3.5×10^5 h^{-1}.

The C_2H_2 and C_2H_4 selectivities on Pt are shown in figure 1(c). The dominant coupling product is C_2H_2, ranging from 7% at 10^5 h^{-1} to 15% at 3.5×10^5 h^{-1}. The selectivity to C_2H_4 was lower at about 4–5% over the entire range of GHSV. C_2H_6 never exceeded 1% carbon atom selectivity, and C_3 and C_4 hydrocarbons were not observed.

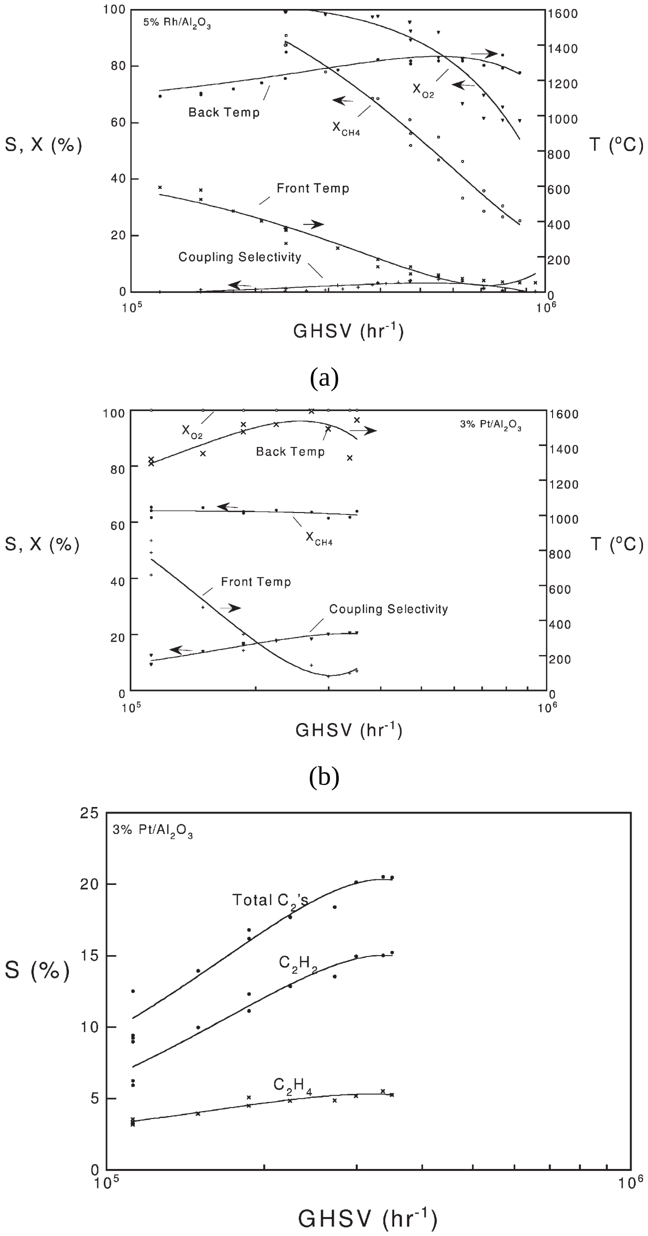

(a)

(b)

(c)

Figure 1. Effect of gas hourly space velocity (GHSV) on methane coupling. Panel (a) shows methane and oxygen conversions, total coupling selectivity, and front and back temperatures vs. GHSV on a 5% Rh/α-Al_2O_3 monolith. Panel (b) shows methane and oxygen conversions, total coupling selectivity, and front and back temperatures vs. GHSV on a 3% Pt/α-Al_2O_3 monolith. Panel (c) shows the total coupling selectivity and acetylene and ethylene selectivities vs. GHSV on a 3% Pt/α-Al_2O_3 monolith.

3.2. Composition

The effect of composition on the coupling selectivity is shown in figure 2 (a) and (b) at a constant GHSV of 1.8×10^5 h^{-1}. The O_2 conversion is complete at CH_4/O_2 ratios below 1.7, however, it decreases at higher ratios to a minimum of 86% at a CH_4/O_2 ratio of 2.4. CH_4 conversion drops from 80% to approximately 30% as the ratio increases from 1.4 to 2.4. The total coupling selectivity decreases from 19% at a ratio of 1.4 to 1% at a ratio of 2.4. The inlet temperature remains nearly constant at approximately 500 °C, while the exit temperature drops from a maximum of around 1500 °C at ratios around 1.7 to 1400 °C at a CH_4/O_2 ratio of 2.4. Figure 2(b) shows that C_2H_2 reaches a maximum of 15% at a CH_4/O_2 of 1.4. C_2H_4 selectivity is at a maximum of 6% at CH_4/O_2 ratios around 1.7, but tails off to a selectivity of 3% at a ratio of 1.4 and 1% at a ratio of 2.4. C_2H_6 has a selectivity of under 1% at a

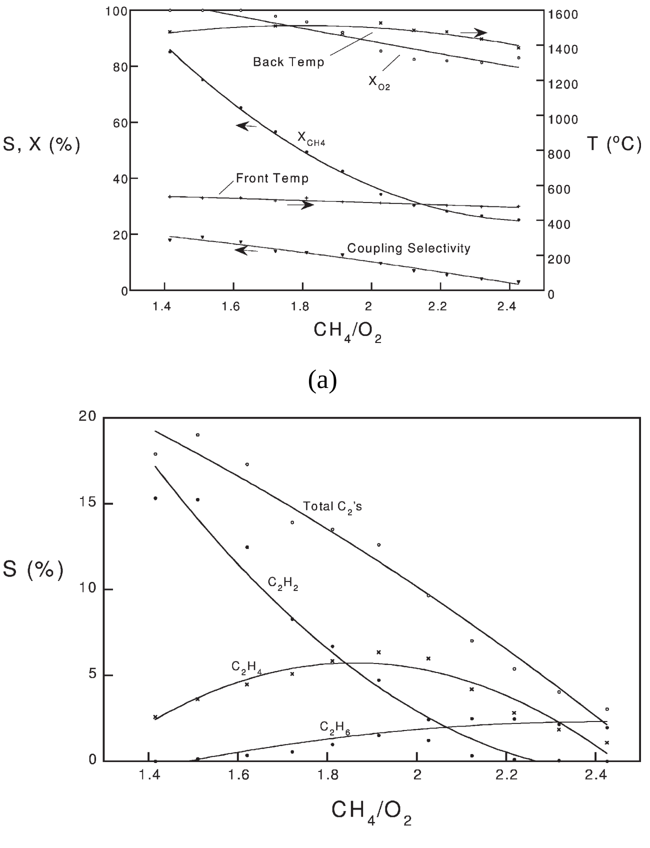

(a)

(b)

Figure 2. Effect of CH_4/O_2 ratio on methane coupling on a 3% Pt/α-Al_2O_3 monolith. Panel (a) shows methane and oxygen conversions, coupling selectivity, and front and back temperatures vs. CH_4/O_2 ratio. Panel (b) shows total coupling selectivity, ethane, ethylene, and acetylene selectivities vs. CH_4/O_2 ratio.

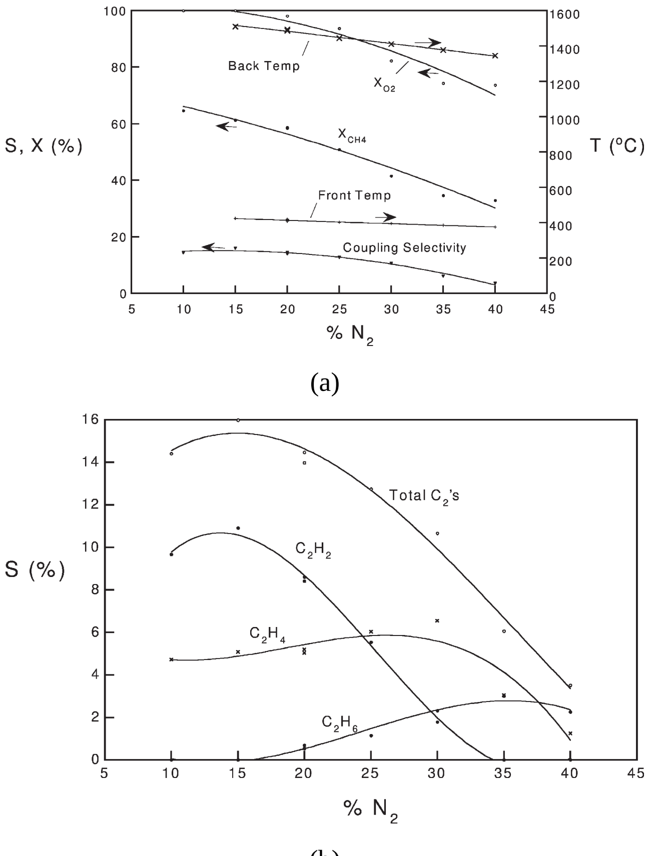

(a)

(b)

Figure 3. Effect of N_2 dilution on methane coupling on a 3% Pt/α-Al_2O_3 monolith. Panel (a) shows methane and oxygen conversions, total coupling selectivity, and front and back temperatures vs. % N_2 diluent. Panel (b) shows total coupling selectivity, ethane, ethylene, and acetylene selectivities vs. % N_2 diluent.

CH_4/O_2 ratio of 1.4, but steadily increases as the CH_4/O_2 ratio increases. It reaches a maximum selectivity of 2.5% at a CH_4/O_2 ratio of 2.4.

3.3. Dilution

To determine the effect of dilution, the amount of N_2 in the feed was varied from 10 to 40%. Below 25% N_2 dilution the O_2 conversion remains complete, but it decreases to less than 80% at 40% dilution, as shown in figure 3(a). The entrance temperature remains relatively constant at approximately 400 °C while the exit temperature decreases from 1500 °C to under 1400 °C as the dilution increases. The total coupling selectivity decreases from a maximum of 16% at 15% N_2 dilution to 4% at 40% dilution.

The selectivities of C_2H_4, C_2H_2 and C_2H_6 are shown in figure 3(b). At dilutions below 25%, C_2H_2 is the dominant C_2, reaching a maximum selectivity of 11% at 15% N_2 dilution. With greater N_2 diluent, C_2H_2 selectivity falls until it is nearly zero at 35% N_2. At N_2 dilutions between 25 and 35%, C_2H_4 is the dominant C_2 with a maximum selectivity of 7% at 30% dilution. C_2H_4 selectivity drops at dilutions higher or lower than 30%, with a selectivity of only 1% at 40% N_2 dilution. The C_2H_6 selectivity increases with increasing dilution, reaching a maximum of 3% with an N_2 dilution of 40%.

Experiments were also done to compare coupling with monoliths of different pore sizes and geometries. An 80 ppi and a 20 ppi monolith were loaded with 6 and 5 wt% Pt, respectively. The 80 ppi monolith resulted in significantly less C_2's than either the 45 ppi or the 20 ppi, with a maximum of 9% at 3.5×10^5 h^{-1}. The 20 ppi monolith produced only 15% coupling selectivity at a maximum, again less than the 45 ppi. Also, when an γ-Al_2O_3 wash-coated α-Al_2O_3 monolith was coated with approximately 2 wt% Pt and run at different flow rates, almost negligible coupling products were produced.

3.4. Stability and homogeneous reactions

As we will discuss, the role of homogeneous reactions may be crucial in interpreting these experiments. At space velocities greater than 2.5×10^5 h^{-1} at a CH_4/O_2 ratio of 1.7, we observed a flame downstream of the catalyst. These flames were typically bright yellow to white and were several millimeters diameter and several inches long in the center of the tube. We never observed flat flames just behind the catalyst, as would be expected if the catalyst acted as a flame holder. Flames were not observed at space velocities less than 2.5×10^5 h^{-1} at any dilution or composition.

High C_2 selectivities were obtained with no evidence of visible flames. When 12 monoliths were placed downstream of the back heat shield to suppress conventional flames, at least 20% C_2 products were obtained at space velocities around 2.5×10^5 h^{-1}. At higher space velocities, the coupling selectivity and methane and oxygen conversions dropped in these experiments. These results suggest that at lower space velocities the observed results are all occurring within the monolith or the back heat shield, but at higher space velocities the flame is responsible for a significant amount of the methane and oxygen conversions and C_2 production.

These experiments have been repeated with more than 100 separate runs on more than 15 different catalysts, with all results consistent with those reported here. However, there was considerable variability in exact conditions where C_2 products were maximized, especially the dependence on flow rates and composition. We suspect that this indicates different roles of homogeneous reactions which vary with specific experiments because of their sensitivity to geometry and temperature profiles.

We also observed no permanent deactivation of any catalysts. Catalysts could be kept in operation for many hours, even in situations where the downstream region of the ceramic monolith appeared to have lost most or all of the Pt.

Carbon buildup was never a problem in these experiments, either from carbon fouling and plugging of the ceramic or heavy buildup of carbon on the walls of the tube after the catalyst. We did observe black films of carbon on the wall of the tube under C_2 forming conditions after minutes of operation, but this occurred several inches downstream of the catalyst where the walls had cooled considerably.

4. Discussion

We suggest that the temperature profile which develops as the space velocity is increased is responsible for the production of acetylene. Figure 4 shows temperature profiles for space velocities around 10^5 h^{-1} and space velocities around 4×10^5 h^{-1} on a Pt-coated monolith. For lower space velocities, the temperature profile in the monolith is fairly flat at around 1000 °C. For the higher space velocities, the temperature profile exhibits a temperature around 200–300 °C at the front of the monolith and a temperature of 1400 °C or higher at the back of the monolith.

For the flat temperature profile at low space velocities, the dominant reaction is the direct partial oxidation of methane to syngas, and less than 0.5% coupling products are observed. The temperature everywhere in the catalyst is too low for gas phase reactions to be significant and too high for carbon to exist on the surface.

For the temperature profile at high space velocities, two possible mechanisms could explain the formation of C_2's from methane under these conditions as sketched at the right of figure 4. The first proposes that a layer of carbon or hydrocarbon absorbs on the colder front region of the monolith, and this carbon layer desorbs through interaction with gaseous species to form the observed coupling products, $C_s + CH_4 \rightarrow C_2H_2 + H_2$. This mechanism is similar to the methane homologation reaction run on Pt at 500–800 °C. The biggest difference is that there is oxygen in our system, which will compete with any coupling reactions on the surface, but which provides the heat to drive the process.

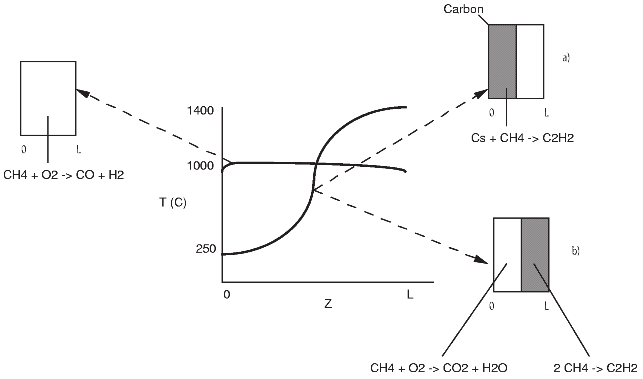

Figure 4. Temperatures profiles for a Pt/α-Al_2O_3 monolith at high and low space velocities, and possible reaction mechanisms for each temperature profile.

The other possible mechanism at these high space velocities is that gas phase reactions occur on the back portion of the monolith where temperatures are in excess of 1400 °C. In this mechanism the colder front region of the monolith catalyzes complete oxidation of CH_4 to CO_2 and H_2O rather than to CO and H_2 because of the lower temperatures. The energy released from this highly exothermic reaction heats up the back of the monolith to temperatures high enough to allow gas phase reactions to compete with surface reactions in this mechanism. Surface reactions lead to partial and complete oxidation, while gas phase reactions produce the observed C_2's.

4.1. Pt vs. Rh

Previously we reported that decreased dilution, decreased CH_4/O_2 ratio and increased GHSV promotes methane coupling over Rh/α-Al_2O_3 [8]. These trends are also observed when Pt is substituted for Rh. However, the total selectivity to C_2's over Pt is at least twice the selectivity observed over Rh. Since the surface of the catalyst may produce CH_3 radicals to feed the homogeneous coupling reaction, Pt may be a better source of CH_3 because of its weaker CH_3–M bond. However, the formation of coupling products may be purely homogeneous, in which case the difference would be that Rh scavenges the CH_3 radicals better than Pt.

Another factor which may explain the differences between the metals is the difference in selectivity towards CO_2 and H_2O on the two metals. Pt has higher selectivities to CO_2 and H_2O than does Rh, meaning that temperatures will generally be much higher on Pt than on Rh and higher temperatures may lead to more coupling products.

4.2. Temperature

In all experiments, the maximum coupling selectivity is observed at the highest catalyst exit temperatures, approximately 1400 °C. At these temperatures, C_2H_2 is a thermodynamically favored product in the absence of oxygen. Flick and Huff have reported similar results in experiments investigating the oxidative dehydrogenation of C_2H_6 [21]. They report acetylene selectivities at a maximum of 16% at a flow rate of 12 slpm, and $C_2H_6/O_2 = 1.2$. In that process C_2H_2 is assumed to form homogeneously when the product gases remain above 800 °C for a critical period of time. The extremely high exit catalyst temperatures observed in our experiments can explain the formation of C_2H_2 in a similar reactor configuration.

The cold initial region of the catalyst may also play an important role in the formation of coupling products. The temperature is approximately 200 °C, low enough to believe the catalyst is extinguished. This allows more unreacted CH_4 to reach the exit of the catalyst. In a secondary role, the cold surface may also act a source of CH_3 radicals which can also further react near the exit of the catalyst. It is also possible that a carbon layer is deposited on this cold surface, and methane or hydrogen interacts with that layer, desorbing C_2 hydrocarbons.

4.3. Role of oxygen in C_2 formation

The production of C_2's was seen for both Pt and Rh at about the same space velocities when oxygen conversion is no longer complete. In addition, greater coupling selectivities are seen with lower CH_4/O_2 ratios. These results suggest a possible relationship between the formation of coupling products and oxygen conversion.

If the hot portion of the monolith is responsible for C_2 formation, it is possible that oxygen is required at the high temperatures for coupling products to form. This makes sense thermodynamically because converting methane to C_2's is unfavorable unless oxygen is present. In addition, if homogeneous reactions are important, oxygen will increase the gas phase reaction rates, possibly allowing them to compete with surface reactions. This suggests that this process can occur only if the monolith reaches a high enough temperature for a long enough period of time in the presence of oxygen.

4.4. Role of monolith geometry

As was mentioned, experiments were run using monoliths with different pore sizes and geometry. Both 20 ppi and 80 ppi monoliths give lower coupling selectivities than the 45 ppi monolith, though 80 ppi gives much lower coupling selectivities. In addition, a wash-coated monolith gave very low coupling selectivities. The main trend appears to be that higher surface areas result in low coupling selectivities because both 80 ppi and a wash-coated monolith have higher surface areas than a 45 ppi monolith. This could be explained by recalling the role of oxygen. A larger surface area will mean that more oxygen is converted in the front of the monolith. This means less oxygen is available to react in the back, hot portion of the monolith which may be the source of the coupling products.

4.5. Model of homogeneous reactions

One possible mechanism for C_2 formation in our process is that methane coupling occurs as a gas phase process, while the primary function of the catalytic monolith is to provide heat necessary for homogeneous reaction to occur. To test this possibility, we modeled our system using a kinetic homogeneous oxidation mechanism developed by Mims and Dean [22] to model gas phase reactions. This model includes 120 species and 447 reactions. It assumes isothermal plug flow with no surface reactions. The Chemkin [23] differential equation solver was used to solve the gas phase differential equations.

Simulations were run at different reaction temperatures using a CH_4/O_2 ratio of 1.7. Figure 5(a) shows a plot of the time to achieve 50% conversion of methane, $t_{1/2}$, versus reaction temperature using only homogeneous reactions. From this figure, we see that at lower temperatures, the ignition time is of the order of hundreds of milliseconds. Not until the temperature is 1200 °C or greater is the ignition time of a similar time scale as our experiments. This suggests that homogeneous reactions are only important when reaction conditions cause a portion of the monolith to heat up to a temperature greater than 1200 °C. This figure also shows that at temperatures of 1400 and 1500 °C, ignition can occur in less than a microsecond, suggesting that it is possible that homogeneous reactions could occur in our system even if the temperature was high for only a fraction of the monolith. It should be noted, however, that surface reactions rapidly deplete O_2 from the gas, and this will decrease the homogeneous reactions.

Selectivities of major products and conversion of oxygen and methane predicted using only homogeneous reactions at 1400 °C are shown versus time in figure 5(b). At extremely short times, when only a small fraction of methane and oxygen have been converted, ethane selectivity rises sharply to a maximum, then decreases rapidly. As the ethane selectivity decreases, the ethylene selectivity increases, reaching a maximum of 36% at a time of 0.4 ms. Ethylene selectivity then drops and selectivity to acetylene rises because of successive dehydrogenation of ethane to ethylene to acetylene.

According to the model, the selectivity to C_2 hydrocarbons increases dramatically at very short times while the selectivities to ethane and ethylene are high and O_2 is still

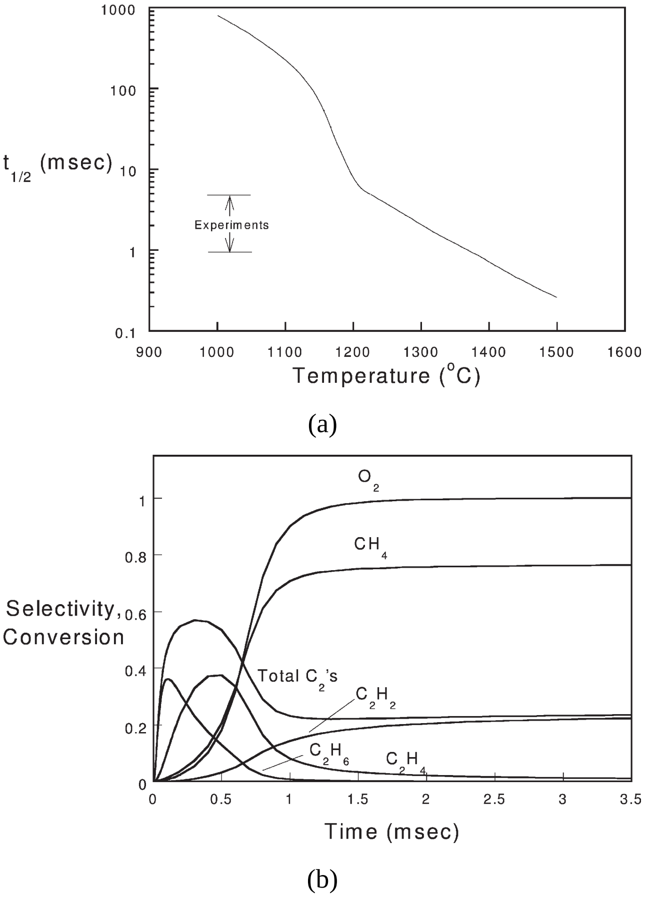

Figure 5. Simulated results assuming a detailed model of homogeneous methane oxidation at $CH_4/O_2 = 1.7$. Panel (a) shows the time for the methane conversion to reach 50% ($t_{1/2}$) vs. temperature. Panel (b) shows methane and oxygen conversions, total coupling selectivities, and ethane, ethylene, and acetylene selectivities vs. time for homogeneous reactions at 1400 °C. For temperatures below 1200 °C little homogeneous reaction is predicted, but above this temperature the times and selectivities to C_2 products are consistent with observed results.

present. It decreases as the ethane and ethylene selectivities drop until 1.2 ms, at which point it begins to increase again as the acetylene selectivity increases. The predicted coupling selectivity through homogeneous reaction alone at millisecond contact times is similar to the experimentally observed selectivity of 20%. At temperatures below 1400 °C, the coupling selectivities are above 20%, with ethylene and ethane as the most prominent C_2's formed, but conversions are low at these millisecond contact times. It should be noted that all of the simulated results are transients. At long times, as equilibrium is approached, few C_2's will exist, as CO and H_2 are the equilibrium products.

Simulations were also run using different methane to oxygen ratios at the same temperature. The homogeneous model predicted higher coupling selectivity with higher methane to oxygen ratios, the opposite of the experimental observations. This indicates that homogeneous chemistry alone cannot account for this trend, or that the experimental results are caused by the higher temperatures that occur using fuel and oxygen mixtures closer to stoichiometric.

5. Summary

The oxidative coupling of CH_4 over Pt yields selectivities of around 20% C_2's at low CH_4/O_2 ratios, low dilution levels and high flow rates. These conditions increase the catalyst exit temperature to nearly 1500 °C, which is high enough that the rates of homogeneous reaction compete with heterogeneous processes. Experimental results were compared to a kinetic homogeneous oxidation model and predicted similar coupling selectivities at millisecond contact times at sufficiently high temperatures, suggesting that homogeneous reactions may be the primary mechanism for C_2 production.

References

[1] A.T. Ashcroft, A.K. Cheetham, J.S. Foord, M.L.H. Green, C.P. Grey, A.J. Murrell and P.D.F. Vernon, Nature 344 (1990) 319.
[2] D.A. Hickman, E.A. Haupfear and L.D. Schmidt, Catal. Lett. 17 (1993) 223.
[3] P.D.F. Vernon, M.L.H. Green, A.K. Cheetham and A.T. Ashcroft, Catal. Lett. 6 (1990) 181.
[4] D.A. Hickman, M. Huff and L.D. Schmidt, Ind. Eng. Chem. Res. 32 (1993) 809.
[5] S.S. Bharadwaj and L.D. Schmidt, Fuel Process. Technol. 42 (1995) 109.
[6] P.M. Torniainen, X. Chu and L.D. Schmidt, J. Catal. 146 (1994) 1.
[7] Y. Wang, P. Witt and L.D. Schmidt, to be published.
[8] P.M. Witt and L.D. Schmidt, J. Catal. 163 (1996) 465.
[9] C.N. Satterfield, *Heterogeneous Catalysis in Industrial Practice*, 2nd Ed. (McGraw-Hill, New York, 1991).
[10] Y. Amenomiya, V.I. Birss, M. Goledzinowski, J. Galuszka and A.R. Sanger, Catal. Rev. Sci. Eng. 32 (1990) 163.
[11] L. Mleczko and M. Baerns, Fuel Process. Technol. 42 (1995) 227.
[12] H. Amariglio, J. Saint-Just and A. Amariglio, Fuel Process. Technol. 42 (1995) 291.
[13] T. Koerts and R.A. van Santen, J. Chem. Soc. Chem. Commun. (1991) 1281.
[14] G.E. Keller and M.M. Bhasin, J. Catal. 73 (1982) 9.
[15] J.M.I. Fox, Catal. Rev. Sci. Eng. 35 (1993) 169.
[16] G. Renesme, J. Saint-Just and Y. Muller, Catal. Today 12 (1992) 371.
[17] J.L. Matherne and G.L. Culp, in: *Methane Conversion by Oxidative Processes, Fundamental and Engineering Aspects*, ed. E.E. Wolf (Van Nostrand Reinhold, New York, 1992) p. 463.
[18] D.A. Hickman and L.D. Schmidt, J. Catal. 136 (1992) 300.
[19] M. Huff, P.M. Torniainen, D.A. Hickman and L.D. Schmidt, in: *Third International Gas Conversion Symposium* (Elsevier, Sydney, 1993).
[20] M. Huff and L.D. Schmidt, J. Phys. Chem. 97 (1993) 11815.
[21] D. Flick and M. Huff, Catal. Lett. 47 (1997) 91.
[22] C.A. Mims, R. Mauti, A.M. Dean and K.D. Rose, J. Phys. Chem. 98 (1994) 13357.
[23] R.J. Kee, F.M. Rupley and J.A. Miller, *Chemkin II: A Fortran Package for the Analysis of Gas Phase Chemical Kinetics*, Sand 89-009 (Sandia National Laboratories, Livermore, CA, 1989).
[24] D.A. Hickman and L.D. Schmidt, J. Catal. 138 (1992) 267.